

Failure stress modification in fatigue life models for rolling bearings

Pradeep K Gupta

Proc IMechE Part J:
J Engineering Tribology
2019, Vol. 233(9) 1327–1344
© IMechE 2019
Article reuse guidelines:
sagepub.com/journals-permissions
DOI: 10.1177/1350650119838895
journals.sagepub.com/home/pij



Abstract

The critical subsurface shear stress related to rolling contact fatigue is modified to model the effects of residual stress common in case hardened materials, such as M50-NiL. The role of hoop stress, generated due to race rotation and shrink fits, is also modeled. It is shown that even relatively low levels of compressive residual stress could contribute to notable increase in bearing life. An equivalent life modification factor is dependent on both residual stress and applied load. Model predictions are in agreement with available experimental life data obtained with a 40-mm angular contact ball bearing with M50-NiL races and silicon nitride balls. The stress modification approach is also applied to model the role of any fatigue limiting shear stress, such that the solutions converge to validated Lundberg–Palmgren solutions as limiting stress reduces to zero. However, bearing life predictions at light loads, under any reasonable limiting stress, are unreasonably high. As an alternate approach, the empirical constant in the limiting stress model, with a prescribed limiting stress, is determined by least-squared regression between model predictions and available experimental life data. With such an approach, the least-squared deviation between model predictions and experimental data shows a monotonic increase as a function of the limiting stress with a minimum at no limiting stress. This observation suggests that simple failure stress modification in the current subsurface stress-based models may not be suitable to implement any fatigue limiting stress for rolling contacts.

Keywords

Rolling contact fatigue, residual stress, fatigue limit, ADORE, rolling element bearing life

Date received: 21 September 2018; accepted: 26 February 2019

Introduction

Based on the classical works of Weibull,^{1,2} the subsurface fatigue process in rolling contacts has been traditionally related to an integral of a function of cyclic subsurface shear stress over the stressed volume. While the widely used, Lundberg–Palmgren (LP) model^{3,4} is based on the maximum orthogonal subsurface stress, Gupta and Zaretsky,⁵ based on earlier work of Zaretsky,^{6,7} have introduced a life model based on maximum subsurface shear stress. In addition, this recent work has generalized the life models in terms of distinct geometrical, materials and operational parameters to present independent life equations for each of the races and rolling elements in terms of contact stress at individual rolling element to race contacts. The individual contact lives are then statistically summed to compute life of the entire bearing. These generalized life equations permit both a change in material properties of bearing elements and simple modification of critical failure stress related to fatigue.

Since the imposed residual and hoop stresses affect the maximum subsurface shear stress, these stresses

certainly affect the bearing fatigue life. Aside from the material processes used in the manufacture of case hardened bearing materials, such as M50-NiL, transformation of retained austenite into martensite during bearing run-in induces significant compressive residual stress which contribute to notable increase in bearing fatigue life, as demonstrated in early pioneering work at General Motors.^{8–12} To further validate the General Motor results, Parker and Zaretsky¹³ made residual stress measurements on several 207-size deep groove ball bearings that were run for different times to establish a suitable pre-stress cycle to induce significant residual stress. The lives obtained with these pre-stressed bearings were found to be twice that of base line bearings under identical applied load and speed conditions. The increase in life due to compressive residual stress is often confused with that

PKG Inc., New York, NY, USA

Corresponding author:

Pradeep K Gupta, PKG Inc., Clifton Park, New York, USA.
Email: guptap@pradeepkguptainc.com

obtained by imposing a fatigue limiting stress. For example, Lorosch,¹⁴ based on full scale life testing, concluded that under low loads with good bearing lubrication there is no material fatigue; however, Zwirlein and Schlicht¹⁵ found significant amount of residual stress due to material transformation in the bearing races used by Lorosch.¹⁴

Bamberger and Kroeger¹⁶ in an experimental investigation reported significant increase in fatigue life with case carburized M50-NiL over the conventional AISI M-50 steel. Also, Townsend and Bamberger¹⁷ used rolling contact test bars to demonstrate significant increase in life in line contact with M50-NiL over AISI 9310. Kotzalas¹⁸ has analyzed the role of residual stress induced during operation on the stress fields used in bearing life predictions. Rosado et al.¹⁹ in experimental life tests with M50-NiL reported only a slight increase in life over AISI M50 but they noted delamination of TiN coating from cage land surfaces leading to damage of race surfaces which could have a detrimental effect on life. More recently, Oswald et al.²⁰ have evaluated the combined role of residual and hoop stresses induced by both bearing speed and interference fit on the races. Modification of critical failure stress to better model the role of residual and hoop stresses in bearing races is the first objective of this investigation.

While Lundberg and Palmgren^{3,4} used the maximum orthogonal subsurface shear stress, and Gupta and Zaretsky⁵ have suggested the use of maximum shear stress, Ioannides and Harris (IH) model²¹ is based on a fatigue limiting stress below which no fatigue may occur and bearing life may be infinite. Although the fatigue limit may be imposed on

any failure stress, Ioannides and Harris²¹ imposed the limit on maximum orthogonal shear stress used by Lundberg and Palmgren.^{3,4} Later Harris and McCool²² implemented the octahedral shear stress, where the fatigue limit may be readily related to the von-Mises stress of applicable bearing material. Harris and Kotzalas²³ have documented the applicable von-Mises stress for several bearing materials. Implementation of a limiting stress in fatigue life models based on subsurface shear stress is evaluated as another application of the critical failure stress modification approach developed in the present effort. Thus, modeling the role of fatigue limiting stress in terms of failure stress modification, and evaluation of the IH model is another objective of this investigation.

Critical failure stresses in life models

The three most common types of subsurface stresses that are used to model rolling contact fatigue are maximum orthogonal shear stress, maximum octahedral shear stress, and the maximum shear stress. For a classical line contact, the variations of these stresses as function of depth below the surface are shown in Figure 1. While the shear stresses are expressed as a ratio, ζ , to the applied contact pressure, the depth coordinate is scaled relative to contact half width and expressed as a ratio, ξ . For convenience, the maximum stress ratios and the corresponding depth ratios are tabulated in Table 1. Although these solutions are for line contact, they may also be applied to point contact in ball bearings, since for most ball bearings, the contact ellipse is fairly narrow with the ratio of major to minor contact ellipse greater than 5.

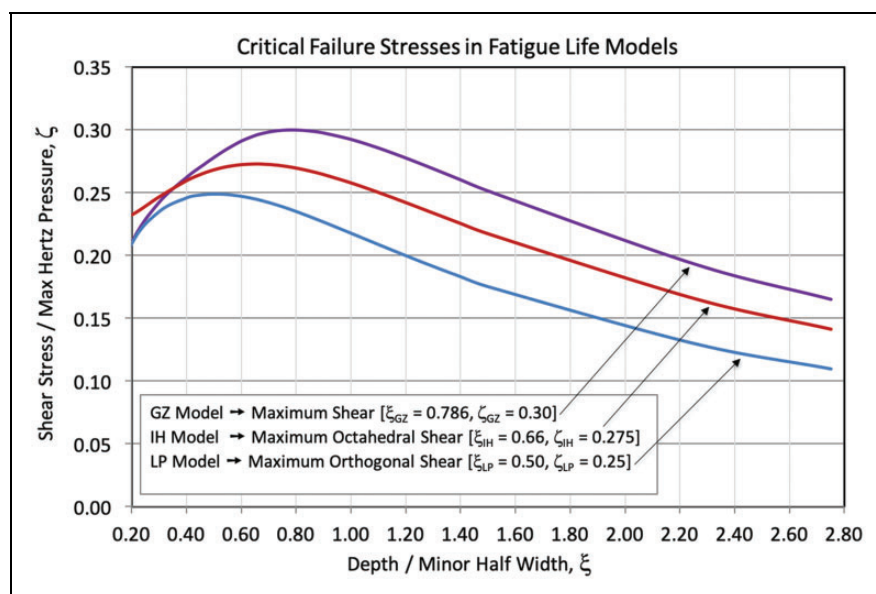


Figure 1. Critical failure stresses used in fatigue life modeling. GZ: Gupta–Zaretsky; IH: Ioannides and Harris; LP: Lundberg–Palmgren.

Table 1. Critical failure stresses in life models.

Stress	$\zeta = \text{Stress}/$ contact pressure	$\xi = \text{Stress}$ depth/ minor contact half width
Maximum orthogonal shear	0.250	0.500
Maximum octahedral shear	0.275	0.660
Maximum shear	0.300	0.786

It may be noted in Table 1 that both the depth and the failure stress are maximum for the maximum shear stress, as is used in the model developed by Gupta and Zaretsky.⁵

Generalized stress–life models

Life models in rolling bearings have traditionally followed the fundamental hypothesis of Weibull,^{1,2} which relates survival probability of a mechanical component, subjected to a cyclic loading, to an integral of a function of the critical failure stress over the stressed volume. With a Weibull modulus m , the expected life, in number of stress cycles, N , is written as

$$\left(\frac{1}{N}\right)^m \sim \int_V f(\tau) V dV \quad (1)$$

Depending on the stress field in a rolling contact, both the definition of a failure stress function and its integration over the relevant subsurface stressed region can be quite complex. In the Lundberg and Palmgren^{3,4} implementation, the applicable stress function is simply assumed as the maximum orthogonal shear stress, τ_o , raised to an empirical exponent, c . Perhaps, the assumption is based on certain rolling contact failures where the spalls appear to be closer to the edge of the Hertzian contact, where the orthogonal shear stress is maximum. The volume of material above maximum orthogonal shear stress and under the Hertzian contact is used as the applicable stressed volume. In addition to the Weibull hypothesis, Lundberg and Palmgren^{3,4} have related the expected life to the depth, z_o , of the maximum orthogonal shear stress raised to another empirical exponent, h . In the development of a life equation, both the failure stress and stressed volume at a given contact are assumed to be constant. With these assumptions, the expected life, L , in units of time, with a contact cycling frequency, u , is written as

$$\left(\frac{1}{L}\right)^m = K \frac{\tau_o^c V_o}{z_o^h} u^m \quad (2)$$

The empirical proportionality constant, K , and the exponents, c and h , are estimated by appropriate analysis of model predictions against experimental life data.

Although the variation of the stress function and the related stressed volume as a function of depth are not explicitly stated in this simplified life relation, these variations are implicit in the empirical constant and exponents, since they are derived by correlating the model predictions to experimental life data.

For practical implementation of the above life equation to a rolling bearing with prescribed geometry and operating conditions, Lundberg and Palmgren^{3,4} carried out the following:

- The Hertzian contact parameters, such as contact pressure and half widths, are related to the applied contact load.
- The maximum orthogonal shear stress and its depth are related first to the Hertzian contact parameters, as shown in Figure 1, and then to the applied contact load.
- Using a Weibull distribution function, a characteristic load under which the bearing could survive one million revolutions with 90% survival probability, is then computed and defined as the dynamic load capacity of the bearing.
- Finally, a simple load–life power relation is stated to compute bearing life at a prescribed load and speed.

In view of its simplicity, this load–life relationship has been the most widely used life model throughout the rolling bearing industry and it is well recognized as the classical LP model. The model is well documented in the text by Harris and Kotzalas.²³ Since at the time of model development the AISI 52100 steel was used for virtually all rolling bearings, constant material properties are included in the empirical constant. The dynamic load capacity is therefore a simple function of operating bearing geometry only.

With the objective of more realistic implementation of the LP model to bearings with varying material properties, Gupta and Zaretsky⁵ have recently generalized the LP model in terms of distinct geometrical and materials parameters, so that the empirical constant is free of any material properties. In addition, the failure stress and stressed volume are more flexibly related to the Hertz contact parameters. This permits more realistic computation of applicable “effective” failure stress and the related stressed volume under arbitrary subsurface stress fields. In particular, the following parameters are introduced:

- Critical failure stress, $\tau = \zeta p_H$
- Depth of critical failure stress, $z = \xi b$
- Width of track for stressed volume computation, $w = \eta a$
- Effective stressed volume, $V \sim dwz \sim \eta \xi dab$
- Materials parameter, $\lambda_E = E'/E'_{52100}$

Here d is the track diameter and E' is the commonly used composite elastic properties parameter

for the two interacting elastic solids, $1/E' = (1 - \nu_1^2)/E_1 + (1 - \nu_2^2)/E_2$. Note that under default Hertzian stress field, the parameters ζ and ξ assume the values specified in Table 1 corresponding to the applicable failure stress. Also, corresponding to the default track width of $2a$, $\eta = 2$.

Unlike the load–life relation in commonly used LP model, Gupta and Zaretsky⁵ have presented a stress–life relation, where the life is related to the Hertzian contact stress. For the present purpose of failure stress modification, the generalized LP life equation is segmented into the stress and stressed volume over depth terms, and written as

$$\frac{1}{L_{LP}} = \frac{(p_H)^{\frac{c}{m}}(p_H)^{\frac{2-h}{m}}}{(p_{HcLP})^{\frac{c+2-h}{m}}} \quad (3)$$

The dynamic stress capacity, p_{HcLP} , contains the empirical constant and the applicable geometrical and materials parameters for the bearing. For race life in ball bearings, the dynamic stress capacity equation is

$$p_{HcLP} = \Phi_{LP} A_{LP} \kappa_{LP}^{-\frac{1}{c+2-h}} \lambda_E^{-\frac{2-h}{c+2-h}} G_{LP}^{-\frac{1}{c+2-h}} u^{-\frac{m}{c+2-h}} \quad (4a)$$

$$\text{Constant, } \kappa_{LP} = \frac{\eta \zeta_{LP}^c \xi_{LP}^{1-h}}{a_1} \quad (4b)$$

$$\text{Reliability factor, } a_1 = \frac{\ln \frac{1}{S}}{\ln \frac{1}{0.90}} \quad (4c)$$

$$\text{Shear stress ratio, } \zeta_{LP} = \frac{\tau_o}{p_H} = 0.25 \text{ (default)} \quad (4d)$$

$$\text{Shear stress depth ratio, } \xi_{LP} = \frac{z_o}{b} = 0.50 \text{ (default)} \quad (4e)$$

$$\text{Contact width ratio, } \eta = \frac{\text{contact width}}{a} = 2 \text{ (default)} \quad (4f)$$

$$\text{Materials parameter, } \lambda_E = \frac{E'}{E'_{52100}} \quad (4g)$$

$$\text{Geometrical parameter, } G_{LP} = d \left(\frac{1}{\sum \rho} \right)^{2-h} a^{*3-h} b^{*3-2h} \quad (4h)$$

$$\text{Cycling frequency, } u = \left| \frac{\Omega - \dot{\theta}}{\Omega_r} \right| \quad (4i)$$

The dynamic stress capacity equation for ball life is essentially identical to the above, except for the geometrical parameter in equation (4h) and cycling

frequency in (4i), are replaced by

$$\text{Geometric parameter, } G_{bLP} = D \left(\frac{1}{\sum \rho} \right)^{2-h} a^{*3-h} b^{*3-2h} \quad (4j)$$

$$\text{Cycling frequency, } u_b = \left| \frac{\omega_b - \dot{\theta}}{\Omega_r} \right| \quad (4k)$$

Note that while the suggested LP values of exponents c and h are retained, the empirical constant A_{LP} is computed by correlating model predictions to experimental data. This constant is related to the fundamental proportionality constant, K , in equation (2). The factor, Φ_{LP} , presently set to 1 (one), is for future use when the empirical constant is modified for further customization of the model.

As a point of validation, Gupta and Zaretsky⁵ have demonstrated that when the applicable material properties are set to AISI 52100 properties at room temperature and with the default values of ζ , ξ and η , as stated above in equations (4d), (4e) and (4f), respectively, the life predictions with the above generalized life model are identical to those estimated by the commonly used load based LP life model.

In addition to the generalization of LP life equation, Gupta and Zaretsky⁵ have presented a new stress-based life equation where data variability in the stress exponent, as seen in LP equation (2) is eliminated, the maximum orthogonal shear stress is replaced by the maximum shear stress, and by postulating rolling contact fatigue as a high-frequency phenomenon, explicit life dependence on depth of the failure stress is eliminated. Thus, the simplified LP equation (2) is modified as

$$\left(\frac{1}{L} \right)^m = K \tau_m^{cm} V_m t^m \quad (5)$$

It may be noted that the above equation conforms more closely to the original Weibull hypothesis stated above in equation (1). Similar to the LP equation, the failure stress and stressed volume may be related to the Hertz contact pressure, and after separating the stress and stressed volume terms, the generalized form of this newly developed Gupta–Zaretsky (GZ) model⁵ is written as

$$\frac{1}{L_{GZ}} = \frac{(p_H)^c (p_H)^{\frac{2}{m}}}{(p_{HcGZ})^{\frac{cm+2}{m}}} \quad (6)$$

Similar to the LP model, the generalized expression for the dynamic stress capacity for race life in ball bearing is written as

$$p_{HcGZ} = \Phi_{GZ} A_{GZ} \kappa_{GZ}^{-\frac{1}{cm+2}} \lambda_E^{-\frac{2}{cm+2}} G_{GZ}^{-\frac{1}{cm+2}} u^{-\frac{m}{cm+2}} \quad (7a)$$

$$\text{Constant, } \kappa_{GZ} = \frac{\eta \zeta_{GZ}^{cm} \xi_{GZ}}{a_1} \quad (7b)$$

$$\text{Shear stress ratio, } \zeta_{GZ} = \frac{\tau_m}{\rho_H} = 0.30 \text{ (default)} \quad (7c)$$

$$\text{Shear stress depth ratio, } \frac{z_m}{b} = \xi_{GZ} = 0.786 \text{ (default)} \quad (7d)$$

$$\text{Geometrical parameter, } G_{GZ} = d \frac{(a^* b^*)^3}{(\sum \rho)^2} \quad (7e)$$

Again, the empirical constant, A_{GZ} , is determined by correlating model predictions to experimental life data. Similar to the LP equation, this constant is related to the fundamental proportionality constant, K , in equation (5). Similarly, the factor, Φ_{GZ} , is for future customization of the empirical constant and is presently set to 1 (one). Also, note that similar to the LP equation, κ_{GZ} , is maintained as a separate constant to permit modification of ζ , ξ , and η for modeling of effective failure stress and stressed volume under applicable stress fields. The contact cycling frequency is same as that defined for the LP model in equation (4i).

The GZ equation for ball life is again identical to the above race life equation, except that equation (4k) is used for the contact cycling frequency, and the geometrical parameter is replaced by

$$\text{Geometric Parameter, } G_{bGZ} = D \frac{(a^* b^*)^3}{(\sum \rho)^2} \quad (7f)$$

Although both the generalized LP and GZ equations presented above use a constant failure stress and stressed volume, they do provide a number of parameters to customize both the effective failure stress and stressed volume under arbitrary stress fields. Also, the effects of variation in failure stress and stressed volume will be implicit in the empirical constant when it is estimated by correlation of model predictions to experimental life data.

Failure stress modification due to residual and hoop stresses

Based on the mechanics of material structure and deformation, residual stress in rolling bearing races may be classified into two different types:

Type 1 residual stress: This type of residual stress is generated by the processes used to manufacture materials, such as case hardened M50-NiL and Pyrowear 675. The stress is present in the newly fabricated races and stays constant as the bearing is subjected to service.

Type 2 residual stress: As the bearing is subjected to contact stress, operating temperatures and repeated cyclic loading, phase transformation of the race material may lead to significant compressive residual stress. This stress is dependent on both the applied loading and the duration of time over which the bearing is in service. Thus, the stress is time dependent. Systematic procedures to define this stress as a function of the required load and time cycles have yet to be developed.

Both types of residual stress generally have a significant variation as a function of depth below the contact surface and the stress fields may be quite complex. However, if the stress fields are well defined, then finite difference or finite element techniques may be used to precisely superimpose these stresses on the subsurface stress field generated by surface loading to determine the applicable integral of the failure stress function over the stressed volume. Generally, these numerical procedures are very compute intensive and they may pose significant practical implementation restrictions in current bearing performance simulation tools, such as ADORE,²⁴ which already require considerable amount of compute power. An alternate approach may be to carry out the complex stress field analysis in isolated cases to define an “effective” failure stress and applicable stress volume which represent the variable stress field. The customized parameters, such as, ζ , ξ , and η , defined in the above generalized life models, may then be used in the bearing performance tools to evaluate bearing performance and life. However, this approach does require systematic development of procedures to determine the subsurface stress fields. Presently, the available data on both Type 1 and Type 2 residual stress are quite limited. Most published data only provide estimated values of these stresses. In view of such limitations, the modeling effort in the present investigation is restricted to constant values of residual stress, as also investigated by Zwirlein and Schlicht.¹⁵ The implementation is also consistent with the development of fundamental subsurface fatigue models, where both the stress function and stressed volume are assumed to be constant. More complex analysis to develop customized effective failure stress and the applicable stressed volume is deferred until more experimental data on residual stress fields becomes available. Thus, the analytical results presented in this investigation provide no more than a guidance to the role of these stresses.

Similar to the residual stress, high-speed bearing rotation and interference fits of the race surfaces contribute to circumferential hoop stress. In addition, thermal expansion of bearing races alters the fits, thereby affecting the hoop stress. Computation of this stress is fortunately quite straight forward. Although this stress also varies with depth, the variation over the relatively small depth of fatigue failure

may be insignificant. Hence, a constant stress value may not be unreasonable to model the role of hoop stress.

While hoop stress in bearing races is in the circumferential direction, residual stress, in addition to the dominant circumferential component, may also have an axial component. The present work only considers purely circumferential stress, which will not produce any orthogonal shear stress. The LP model based on maximum orthogonal shear stress, as formulated above, is therefore insensitive to such stress modifications. However, the circumferential stress will generate maximum shear stress, as used in the GZ model, so it may be superimposed on the stress generated due to applied surface loading. Thus, in the present investigation, modeling of residual and hoop stresses is restricted to the GZ model.

The maximum shear stress produced by prescribed values of residual and hoop stresses will only affect the magnitude of the failure stress and the depth at which the maximum occurs will be unaffected. This is also demonstrated by Zwirlein and Schlicht.¹⁵ Thus, only the stress term in the GZ equation (6) is modified, and the volume term remains unchanged. If σ_r is the residual stress and σ_h is the hoop stress, then the equivalent maximum shear generated by these stresses may be written as

$$\tau_e = \pm \frac{\sigma_r}{2} \pm \frac{\sigma_h}{2} \quad (8)$$

where the positive and negative signs correspond to tensile and compressive stress respectively.

Using the maximum shear to Hertz pressure ratio, ζ_{GZ} , as defined above for the GZ model, the pressure term corresponding to the maximum shear stress variation in the life equation (6) may be modified as

$$\frac{1}{L_{GZ}} = \frac{\left(p_H \pm \frac{\sigma_r}{2\zeta_{GZ}} \pm \frac{\sigma_h}{2\zeta_{GZ}} \right)^c (p_H)^{\frac{2}{m}}}{(p_{HcGZ})^{\frac{cm+2}{m}}} \quad (9)$$

If L_{GZ0} is the contact life without any stress modification, then the life after shear stress modification as a result of residual and hoop stresses may be written as

$$\frac{1}{L_{GZ}} = \frac{1}{L_{GZ0}} \left[1 \pm \frac{\sigma_r}{2p_H\zeta_{GZ}} \pm \frac{\sigma_h}{2p_H\zeta_{GZ}} \right]^c \quad (10)$$

When the expression within the brackets is zero or negative, the modified life is infinite. The above life modification may also be expressed in terms of a life modification factor, ψ_R , applied on the life computed without any residual or hoop stress.

$$L_{GZ} = \psi_R L_{GZ0} \quad (11a)$$

$$\psi_R = \left[1 \pm \frac{\sigma_r}{2p_H\zeta_{GZ}} \pm \frac{\sigma_h}{2p_H\zeta_{GZ}} \right]^{-c} \quad (11b)$$

In order to demonstrate the practical significance of such a life modification approach, the above life modification is implemented in the bearing dynamics code ADORE,²⁴ along with the base life equations. Bearing life is then predicted for a 40-mm angular contact ball bearing, used earlier by Rosado et al.¹⁹ to model the GZ bearing life as a function of applied load, or inner race contact stress, with varying levels of compressive residual stress in both races. The bearing operates at a shaft speed of 10,000 r/min with the outer race temperature of 400 K. At this operating speed, for the size of this bearing, the hoop stress is found to be negligible, although this stress is accounted for in the calculation. Race material for both races is M50-NiL, while the material for the balls is silicon nitride. Nominal bearing geometry is documented in Table 2.

For case hardened materials, such as M50-NiL, a variation in elastic modulus as a function of depth has been reported. The modulus is highest at the surface, and it gradually reduces to the nominal modulus of the base material as a function of depth. Klecka et al.²⁵ have measured such an elastic modulus variation in M50-NiL steel. In order to realistically model the effect of such elastic modulus variation, a rigorous analysis of both the contact problem and subsurface stress field is required. As a first approximation, since elastic deformation varies inversely as cube root of the elastic modulus, the current work uses a cube root average of the elastic modulus over the core depth. This provides an effective elastic modulus slightly higher than that of the base material M50. Very recently, Londhe et al.²⁶ have carried out a finite element analysis of ball/race contact with varying elastic modulus in the race material. By matching the Hertz contact stress for the case hardened material with that obtained with an equivalent through hardened material, they have provided a regression procedure to compute an effective elastic modulus. The

Table 2. M50-NiL hybrid ball bearing geometry.

Bearing bore	40 mm	Pitch diameter	60.25 mm
Bearing OD	80 mm	Contact angle	22°
Number of balls	11	Outer race curvature factor	0.52
Ball diameter	12.70 mm	Inner race curvature factor	0.52

effective modulus so computed is also slightly higher than that of the base through hardened material, and it is very much in line with the simplified assumption stated above. The slightly higher elastic modulus provides approximately 3% increase in the Hertz contact pressure, which actually leads to a reduction in fatigue life. In spite of this reduction in life, Londhe et al.²⁶ have attributed the generally improved performance of case hardened materials to significant residual stress build up in the material as a result of the manufacturing process. Aside from elastic modulus variation in the core, a more significant change in elastic modulus is actually as a function of temperature, when the elastic modulus drops with increasing temperature. In the range of typical operating temperatures in turbine engine bearings, such a drop in elastic modulus leads to a notable increase in bearing fatigue life.⁵ In the present investigation, in addition to the modulus variation as a function of core depth, the elastic modulus is also corrected for thermal effects using the available data for M50 VIMVAR bearing steel.²⁷

The test bearing materials, geometry, and operating conditions are identical to those used by Rosado et al.¹⁹ in their experimental investigation.

The bearings are not subjected to any mounting fits, which could generate significant hoop stress. The analytical life predictions with the above failure stress modifications are shown in Figure 2. Experimental life data for the 40-mm hybrid bearing obtained by Rosado et al.,¹⁹ along with more recent data published by Trivedi et al.²⁸ are summarized in Table 3. In both these data sets, residual stress measurements are carried out on fresh races; thus, they are Type 1 residual stresses. Since the analytical models predict basic subsurface life, the actual life measured experimentally must be reduced by applicable life modification factors under the experimental operating conditions. The most commonly used life factors, after the ISO publication in 1989,²⁹ are the STLE recommended factors,³⁰ and the more comprehensive life modification factors developed by Tallian.³¹ Rosado et al.¹⁹ used the STLE life modification factors,³⁰ which include factors for materials, processing and lubrication, referred to a_2 and a_3 factors in the ISO standard.²⁹ The applicable STLE factors are also listed in Table 3. As shown in Figure 2, the Rosado et al.¹⁹ experimental point falls just above the no residual stress predictions, although compressive residual stress is reported to be in the range of 100 to 300 MPa.

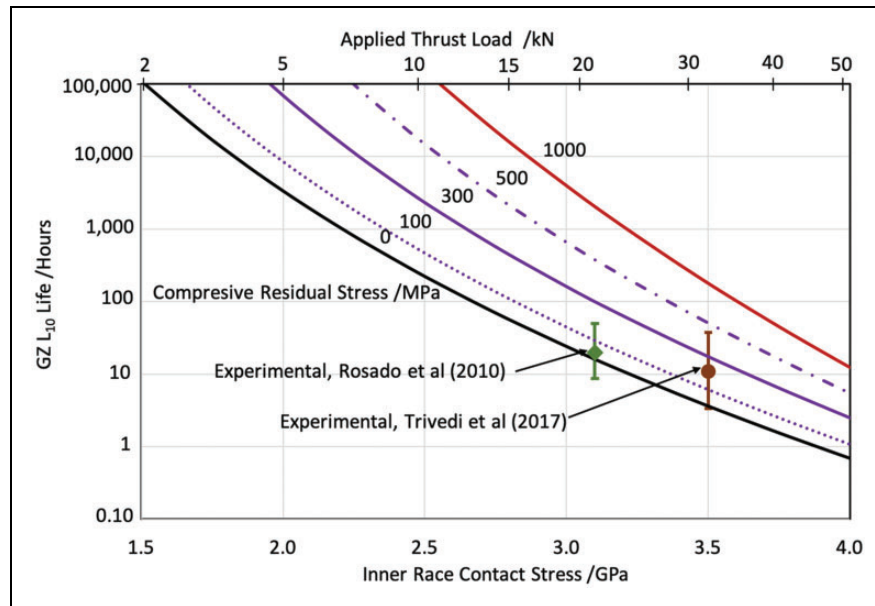


Figure 2. Parametric GZ life predictions for a 40-mm M50-NiL hybrid ball bearing as a function of compressive residual stress and applied load for a 40-mm hybrid ball bearing operating at 10,000 r/min at 400 K. GZ: Gupta–Zaretsky.

Table 3. Experimental data for the 40-mm hybrid ball bearing.

Data set	Inner race contact stress (GPa)	Failure index	Experimental life (h)	STLE life modification factor	Estimated basic L_{10} life (h)
Rosado et al. ¹⁹	3.1	4/10	774	39	19.85
Trivedi et al. ²⁸	3.5	8/16	422.4	38	11.11

However, based on visual examination of the failed bearings, Rosado et al.¹⁹ have reported delamination of TiN coating on the cage guidance lands and some damage to the race surfaces. Although a precise mode of failure is not included in the published work, it is speculated that the observed damage to race surfaces may have accelerated failure propagation. Thus, the correlation between model prediction and experimental data obtained by Rosado et al.¹⁹ may not be unreasonable.

Trivedi et al.²⁸ have presented another data set for the 40-mm hybrid ball bearing. Except for the race curvature factors, which are modified to 0.53, geometry of the bearing is identical to that used by Rosado et al.¹⁹ The increased race curvature factors produce a slightly higher contact stress under the operating conditions identical to those used by Rosado et al.¹⁹ The experimental point corresponding to this data set, as summarized in Table 3, and plotted in Figure 2, falls right in the range of model predictions corresponding to the expected range of residual stress. Thus, the model prediction is in good agreement with experimental data.

Alternatively, the results of Figure 2 may be replotted in Figure 3 in terms of a life modification factor defined in equation (11b). It should be noted that at light applied loads and high levels of compressive residual stress, the bearing life may become infinite. Also, the life modification factor is both residual stress and applied load dependent.

Failure stress modification due to fatigue limiting stress

Ioannides and Harris²¹ have proposed infinite bearing life when applied stress is below a prescribed fatigue

limiting stress. The limiting stress is imposed on the orthogonal shear stress, used by Lundberg and Palmgren^{3,4} such that the bearing life is infinite when the maximum orthogonal shear stress due to applied loading is less than the fatigue limiting stress. When the applied maximum orthogonal shear stress is greater than the limiting stress, then the effective failure stress is reduced by the limiting stress. When the limiting stress is reduced to zero the predicted life converges to that obtained by the LP model. In other words, the LP empirical constant in the life equation is retained. A few years later, Harris and McCool²² replaced the maximum orthogonal shear stress with the maximum octahedral shear stress and applied the limit on the octahedral stress. This limiting stress is related to the von-Mises stress, which has been documented for several bearing materials by Harris and Kotzalas.²³ Subsequent to these limiting stress models, the International Standards Organization (ISO) has published the ISO 281 standard³² which suggests a limit stress for fatigue life modeling corresponding to a maximum contact stress of 1.5 GPa.

Primarily, due to the lack of experimental evidence establishing the existence of a limiting stress in rolling contact fatigue, life models based on limiting stress have been quite contentious.³³⁻⁴¹ Carrying out actual life tests at light loads, which could possibly lead to infinite life, is quite difficult and perhaps expensive. Thus, in the present work, with the assumption that a fatigue limiting stress does exist, the applicable failure stress is simply modified by a limiting stress and the impact on life is modeled. The approach is identical to that used above for the residual and hoop stresses,

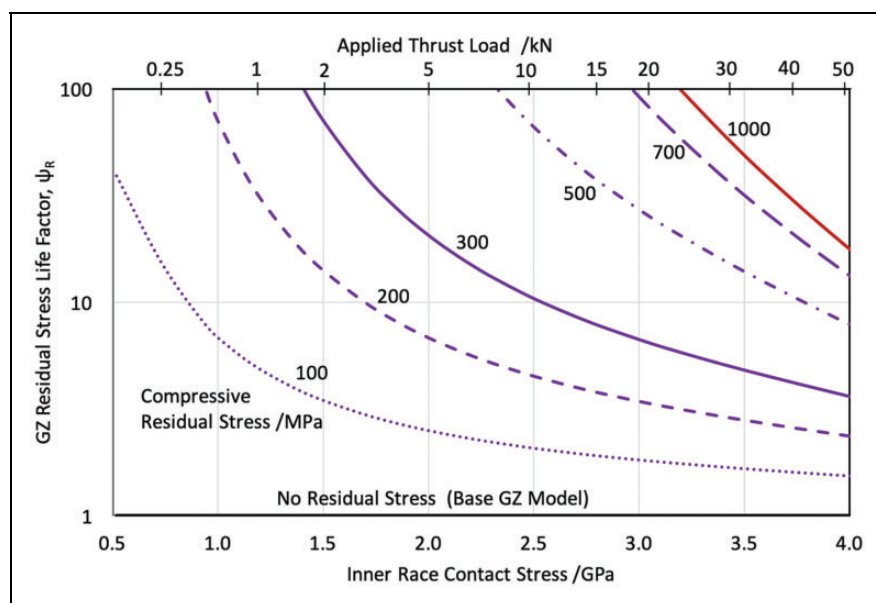


Figure 3. The impact of compressive residual stress in bearing races of a 40-mm M50-NiL hybrid ball bearing operating at 10,000 r/min and 400 K.

GZ: Gupta–Zaretsky.

except for the implementation of fatigue limit both the stress and volume terms are modified, since the life model only applies when the stress is above the prescribed limiting stress.

Ioannides and Harris²¹ carried out a fairly rigorous integration of the modified stress function over the stressed volume. However, the empirical constant in the life equation is still estimated by matching the predicted dynamic capacity to the LP value, as the limiting stress is reduced to zero. Thus, consistent with the LP development, it may not be unreasonable to simply implement a constant modified stress function over a prescribed volume to model the effect of limiting stress. Also, in order to maintain the flexibility to add the residual and hoop stresses in the limiting stress model, the orthogonal stress, used by Lundberg and Palmgren,^{3,4} is replaced by octahedral shear stress, as done by Harris and McCool.²² Therefore, implementation of IH model in the present investigation is carried out in two parts:

- In the LP model, the maximum orthogonal shear stress is replaced by maximum octahedral shear stress, and the empirical constant is recalibrated with available experimental data. Thus, the predicted life with octahedral based stress is identical to that obtained by the original orthogonal shear stress-based model.
- A limiting octahedral stress for the specified bearing material is then imposed to modify both the effective failure stress and stressed volume. The limiting stress is related to the von-Mises stress documented by Harris and Kotzalas.²³ When the operating octahedral stress is less than this limiting stress, the bearing life is infinite.

Thus, the orthogonal shear stress, τ_o , in LP equation (2), is replaced by an octahedral shear stress, τ_{oct} , which may be defined as

$$\tau_{oct} = \zeta_{IH} p_H \quad (12a)$$

where ζ_{IH} is the ratio of octahedral shear stress to contact pressure, as tabulated in Table 1. The failure stress is then modified by subtracting a fatigue limiting stress τ_l , which is defined as

$$\tau_l = \frac{\sqrt{2}}{3} \sigma_v \quad (12b)$$

where σ_v is the von-Mises stress for the prescribed bearing material, as tabulated by Harris and Kotzalas.²³

Since the modified life equation is now based on octahedral stress, the failure stress modification due to residual and hoop stress may also be applied. While the limiting stress effect is applied to all parts of the life equation, stress modification due to residual and hoop stresses is only applied to the stress part of the

equation, as done above in the GZ model. Thus, based on the LP life equation (3), the IH life equation is written as

$$\frac{1}{L_{IH}} = \frac{\left(p_H - \frac{\varphi \tau_l}{\zeta_{IH}} \pm \frac{\sqrt{2} \sigma_r}{3 \zeta_{IH}} \pm \frac{\sqrt{2} \sigma_h}{3 \zeta_{IH}} \right)^{\frac{c}{m}} \left(p_H - \frac{\varphi \tau_l}{\zeta_{IH}} \right)^{\frac{2-h}{m}}}{(p_{HcIH})^{\frac{c+2-h}{m}}} \quad (13)$$

Here, φ is introduced as an arbitrary limiting stress modifier, which could be assigned an arbitrary value. A value of 1 (one) represents the IH model when the limiting shear stress corresponds to the von-Mises stress for the specified bearing material; a value of 0 (zero) removes the limiting stress and reduces the IH model to LP model with maximum octahedral shear stress as the critical failure stress. Similar to the LP and GZ models, the dynamic stress capability, p_{HcIH} , contains an empirical constant, A_{IH} , which is derived by fitting model predictions under no limiting stress to available experimental life data.

As done in the failure stress modification for the GZ model, the IH life may also be expressed in terms of a base IH life, L_{IH0} , with no stress modification, as

$$\frac{1}{L_{IH}} = \frac{1}{L_{IH0}} \left[1 - \frac{\varphi \tau_l}{p_H \zeta_{IH}} \pm \frac{\sqrt{2} \sigma_r}{3 p_H \zeta_{IH}} \pm \frac{\sqrt{2} \sigma_h}{3 p_H \zeta_{IH}} \right]^{\frac{c}{m}} \times \left[1 - \frac{\varphi \tau_l}{p_H \zeta_{IH}} \right]^{\frac{2-h}{m}} \quad (14a)$$

$$\frac{1}{L_{IH0}} = \left(\frac{p_H}{p_{HcIH}} \right)^{\frac{c+2-h}{m}} \quad (14b)$$

Note that equation (14b) is identical to the LP equation (3), except that the failure stress is the maximum octahedral stress.

When the residual and hoop stress components are neglected, equations (14a) and (14b) may be expressed in terms of a limiting stress life factor, ψ_S , as

$$L_{IH} = \psi_S L_{IH0} \quad (15a)$$

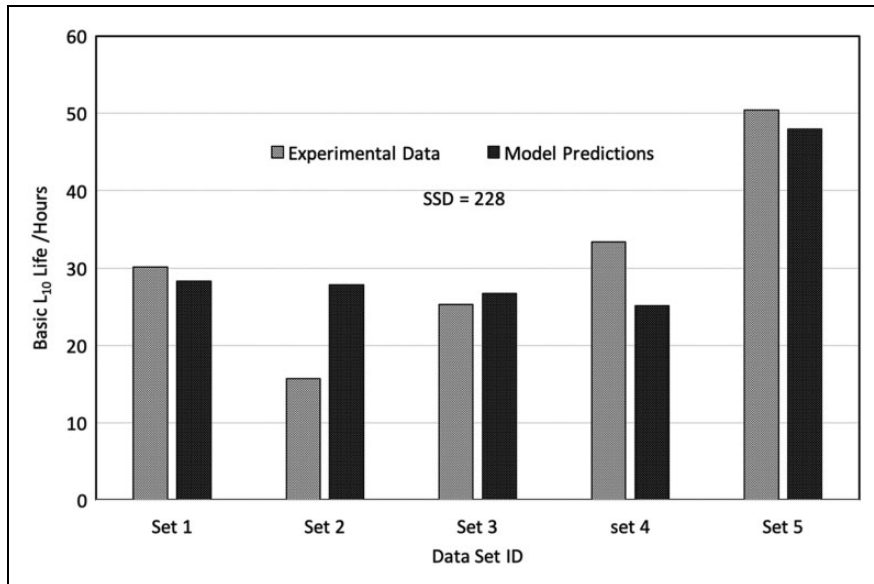
$$\psi_S = \left[1 - \frac{\varphi \tau_l}{p_H \zeta_{IH}} \right]^{\frac{c+2-h}{m}} \quad (15b)$$

For parametric evaluation, the model is again implemented in the bearing dynamics code, ADORE.²⁴

The five experimental data sets used by Gupta and Zaretsky⁵ to compute the model constants in the generalized LP and newly introduced GZ models are also used to compute the model constant in the IH model. The contact stresses and failure indices in these five data sets are reproduced in Table 4. As a first step of IH model implementation, the orthogonal shear stress in the LP model is replaced by octahedral shear stress and the model is fitted to the experimental data to derive the applicable base constant. This defines the

Table 4. Experimental life data obtained with a 120 mm angular contact ball bearing.

Data set ID	Inner race contact stress (GPa)	Failure index	Applicable life modification factor	Estimated basic L_{10} life (h)
Set 1	2.35	10/27	6.51	30.1
Set 2	2.35	14/27	6.39	15.67
Set 3	2.36	11/26	6.15	25.30
Set 4	2.38	6/26	6.48	33.33
Set 5	1.95	6/30	30.46	50.39

**Figure 4.** Least-squared regression fit of the IH model predictions to the experimental data sets under no limiting stress. The model converges to LP predictions with maximum octahedral shear as the failure stress.**Table 5.** AISI 52100 ball bearing geometry.

Bearing bore	40 mm	Pitch diameter	66.040 mm
Bearing OD	80 mm	Contact angle	15°
Number of balls	13	Outer race curvature factor	0.525
Ball diameter	11.100 mm	Inner race curvature Factor	0.535

base LP model with octahedral shear stress, which is also the limiting solution for the IH model when the stress limit is reduced to zero. The model fit is shown in Figure 4. Note the Sum of squared deviation (SSD) is also shown in Figure 4. This value indicates the level of fit between model predictions and experimental data. Discussion on significance of this value follows later in the article.

Once the model constant is established via regression analysis, model predictions with the IH model, with a prescribed stress limit, may be compared with the LP and GZ models. For this purpose, another 40-mm ball bearing operating at 10,000 r/min is again used with the operating temperature set to 293 K (room temperature). The bearing geometry is

tabulated in Table 5. The material of both races and the balls is set to AISI 52100 steel in order to obtain a fair comparison with the original LP model.

Life predictions, as obtained by the various models, are shown in Figure 5; note that the generalized LP and the original LP solutions are identical, since the bearing material is AISI 52100 bearing steel at room temperature. Simply to evaluate the role of limiting stress, the residual and hoop stress components are set to zero in these parametric runs. The limiting stress in the IH model is derived from the von-Mises stress for AISI 52100 steel as tabulated by Harris and Kotzalas²³; the stress limit modifier, ϕ , is 1.0 under this condition. At low stresses, the GZ predictions are about an order of magnitude higher in

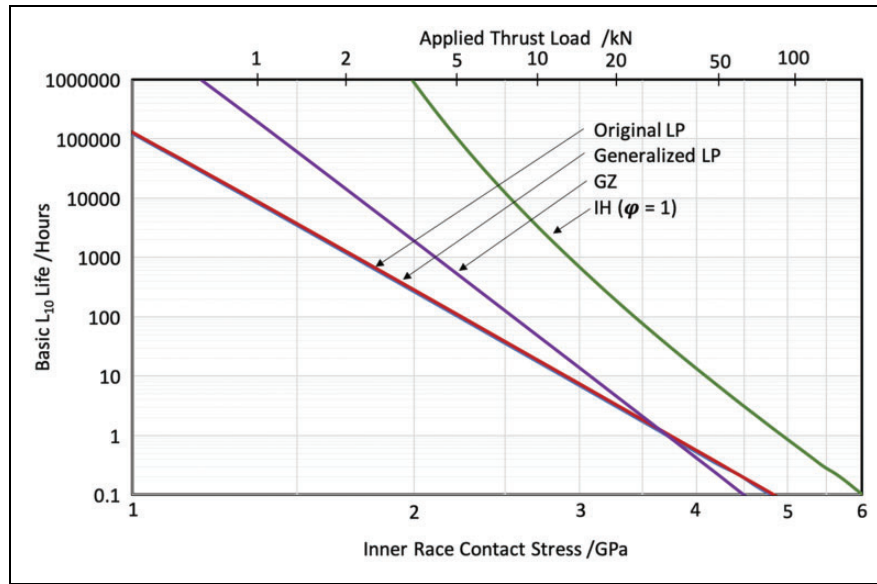


Figure 5. Comparison of life predictions with the various life models for the 40 mm AISI 52100 ball bearing operating at 10,000 r/min at room temperature.
LP: Lundberg–Palmgren.

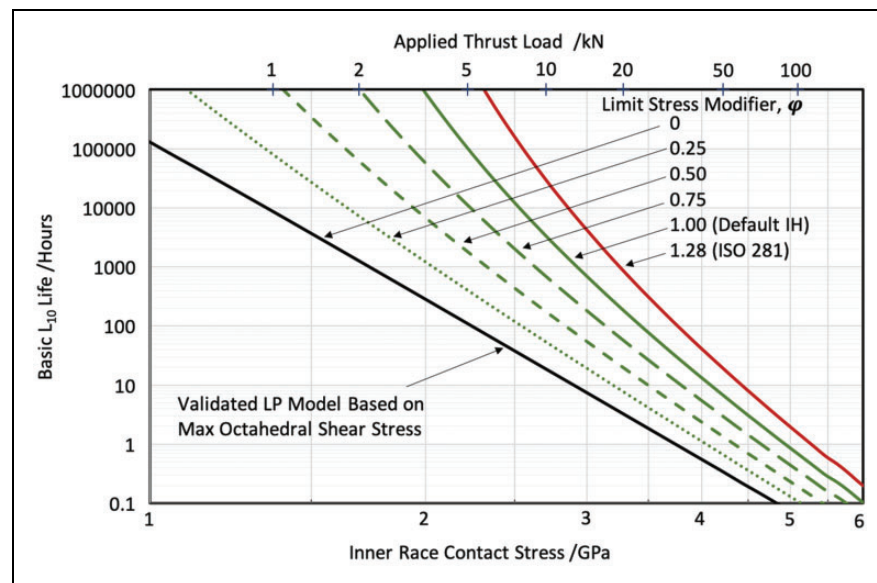


Figure 6. Parametric life predictions of fatigue limiting stress-based IH life model.
LP: Lundberg–Palmgren.

comparison to the LP model, while the predictions are lower at high contact stresses. This is due to a higher stress–life exponent in the GZ model as discussed by Gupta and Zaretsky.⁵ With the IH model, however, the life predictions are greatly higher, particularly at low stresses. Also, the stress–life relation is no longer linear on a logarithmic scale, as expected from equation (13).

In order to elaborate on the significance of limiting stress in life predictions, parametric solutions are obtained with the IH model with varying limiting

stress, including the ISO 281³² suggested fatigue limiting stress corresponding to a Hertz contact stress of 1.5 GPa. For the AISI 52100 bearing steel, and with a maximum octahedral to Hertz contact pressure ratio of 0.275, this corresponds to a limiting stress modifier, ϕ , of 1.28. In other words, ISO 281 suggests a limiting stress is 28% higher than that proposed by Ioannides and Harris.²¹ The parametric results of IH model predictions with varying values of limiting stress modifier, ϕ , are shown in Figure 6. Both the predicted lives at low stress levels and the rate of life increase with

reducing stress are highest with the ISO standard. As the stress limit modifier is reduced, the predicted lives, particularly at low stresses, reduce rapidly and the stress–life relationship becomes increasingly linear. When the limiting stress modifier is set to zero, the relationship becomes linear, and the model converges to the LP stress–life relation. While the LP model uses the maximum orthogonal shear stress, and IH model uses maximum octahedral shear stress, the overall impact on life with these two formulations is just a change in scale factor, which is part of the model constant determined by regression analysis of experimental data. Therefore, the two solutions are essentially coincident.

In absence of any residual or hoop stress effects, the solutions of Figure 6 may be presented in terms of the limiting stress life factor, defined earlier in equation (15b). This is done in Figure 7. Since the IH model converges to the LP solutions with no limiting stress, these solutions may be applied on the currently used LP model to assess the role of limiting stress on bearing life. Clearly, the predicted lives with the limiting stress-based models, based on the classical LP equation via simple failure stress modification, are orders of magnitude higher than those obtained with the base LP model. Such a strong dependence of life on limiting stress makes the applicable limiting stress very critical in the life models. It may be quite possible that in the event, a fatigue limiting stress does exist for rolling contact; then the fundamental subsurface fatigue hypothesis formulated by Lundberg and Palmgren,^{3,4} is no longer applicable and based on experimental support, development of an alternate fatigue hypothesis may be necessary.

A numerical experiment

Full scale rolling bearing life tests at light loads are extremely difficult and perhaps quite expensive. Therefore, it may be difficult to experimentally establish a fatigue limiting stress in rolling contacts, similar to the one established in simple bending or torsion. However, in order to make some assessment of the significance of limiting stress in life modeling, a “numerical experiment” is carried out, with the following assumptions:

1. A viable fatigue limiting stress does exist for rolling contacts.
2. Applicable limiting stress is somewhat of an unknown.
3. Similar to the classical subsurface fatigue, the fundamental hypothesis in the fatigue limiting stress-based model still consists of stress–volume integration, except that the applicable failure stress is reduced by the limiting stress.
4. Like any other model, life predictions with a prescribed limiting stress model must agree reasonably well with experimental life data under a stress above the limiting stress when the bearings do fail.

In view of assumptions (1) and (2), the life model is formulated in terms of a variable limiting stress, as already done above in terms of the limiting stress modifier, φ . In accordance with assumption (3), the model is based on the well-established LP model, except that the applicable failure stress is reduced by the limiting stress. This is also already done in the formulation presented above. Finally, conforming to

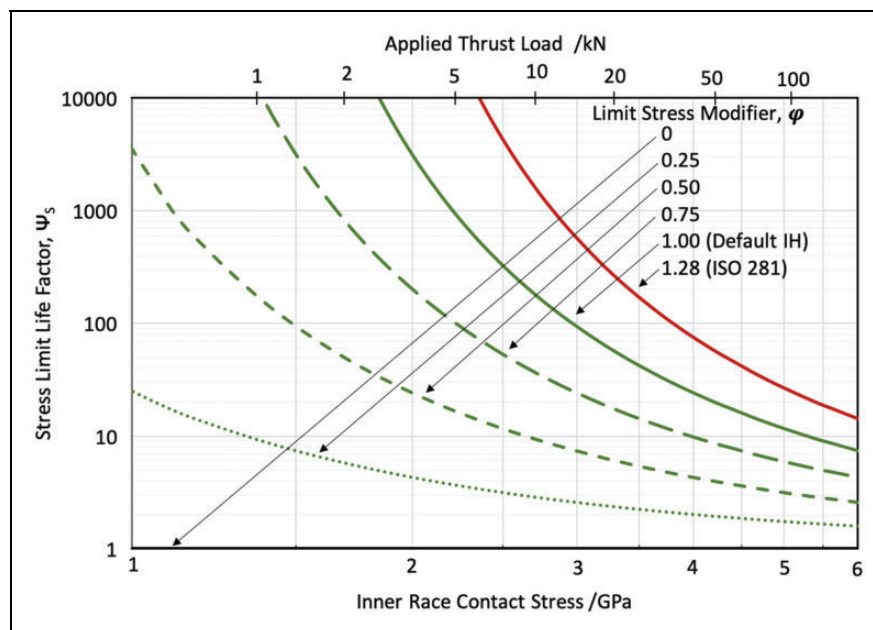


Figure 7. Estimated life factors for fatigue limiting stress as a function of the limiting stress and the applied load for the 40 mm AISI 52100 ball bearing operating at 10,000 r/min at room temperature.

assumption (4), for a given value of φ , a least-squared deviation analysis of model predictions against available experimental data is carried out to estimate the applicable empirical model constant. Such a process makes the model constant dependent on prescribed fatigue limiting stress, but model predictions agree reasonably well with experimental life data under stresses greater than the fatigue limiting stress when the bearings do fail.

Using the above approach, IH model correlations, at a limiting stress corresponding to the von-Mises stress of the material ($\varphi = 1$), with the five

experimental data sets, documented in Table 4, are shown in Figure 8. The figure also documents the minimum value SSD (sum of squared deviation between model predictions and experimental data). Comparing this SSD value with the corresponding value at no limiting stress (documented earlier in Figure 4) reveals that the model fit is better at no limiting stress.

Again, using the 40-mm bearing with AISI 52100 bearing steel, comparisons of life predictions with the above fatigue limiting stress model are compared with the LP solutions in Figure 9. Although the model predictions are now similar around the experimental

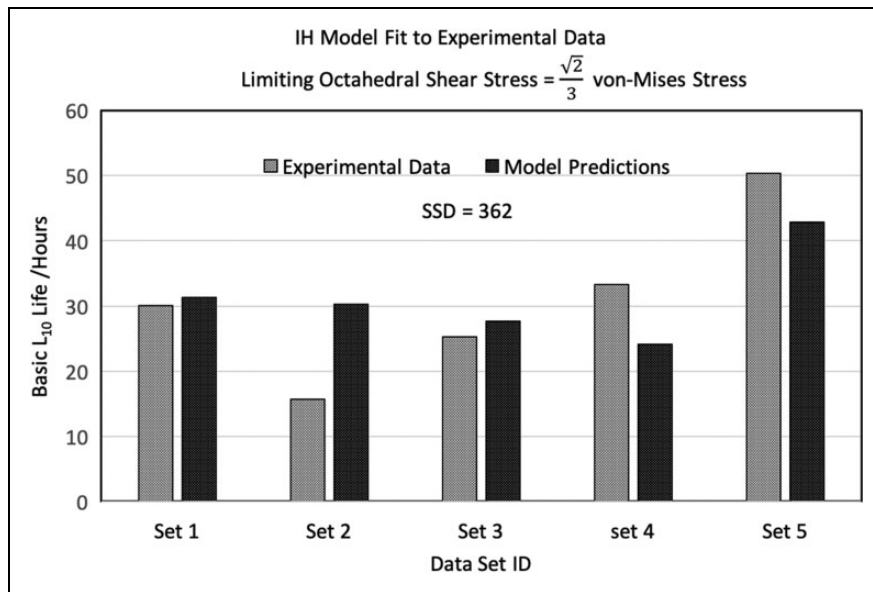


Figure 8. IH model correlation with experimental data at the fatigue limiting octahedral shear stress corresponding to the von-Mises stress of the material.

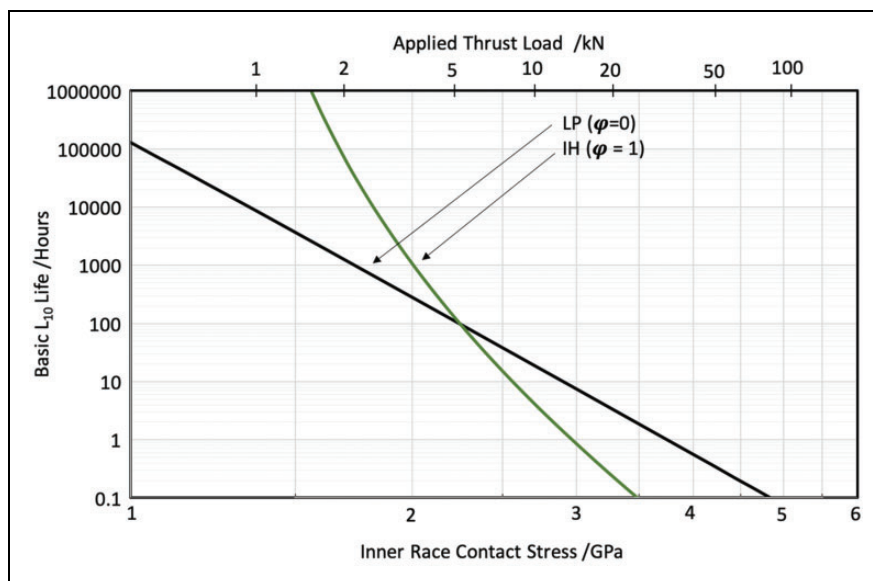


Figure 9. Comparison of IH and LP life predictions, for the 40 mm AISI 52100 ball bearing operating at 10,000 at room temperature, with IH model constant obtained by independent correlation with experimental life data. IH: Ioannides and Harris; LP: Lundberg–Palmgren.

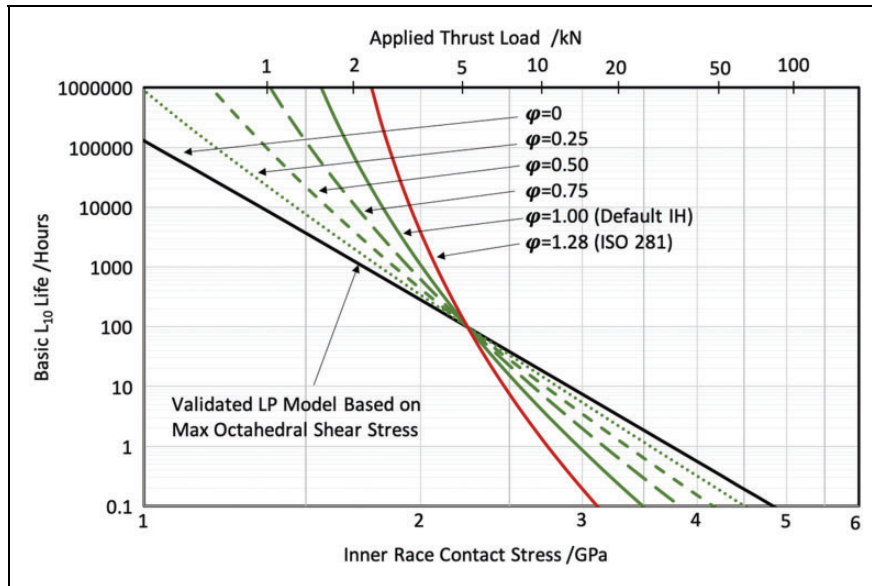


Figure 10. Parametric life predictions for the 40 mm AISI 52100 ball bearing, operating at 10,000 r/min at room temperature with varying levels of fatigue limiting stress.

LP: Lundberg–Palmgren.

stress points, the IH lives are substantially higher at low stress levels and lower at high stresses in comparison to the LP predictions.

The above analysis is repeated at varying values of limiting stress, including the ISO 281 recommendation, and life prediction is plotted as a function of applied load on the bearing. Again the 40-mm bearing with AISI 52100 bearing steel is used to produce the results shown in Figure 10. As the limiting stress reduces to zero, the model converges to the LP solution. Note that all solutions intersect at a stress point between 2 and 2.5 GPa. This happens to be an effective stress for the five experimental data sets, documented earlier in Table 4. If the experimental data were available at a wider range of applied contact stress, then this point of intersection may vary. Interestingly, these results are qualitatively identical to the results published by Ioannides and Harris²¹ for rotating beams.

Finally, to evaluate the model fit to experimental data and determine an optimum value of φ , the computed SSD with a model with limiting stress modifier, φ , relative to the SSD obtained with a model with no limiting stress is plotted as a function of the prescribed limiting stress, or the limiting stress modifier in Figure 11. Note that this SSD ratio may also be interpreted as a ratio of more commonly used RMS deviation. As stated earlier, the factors of 1.28 and 1, respectively, correspond to the ISO 281 standard and the IH model with limiting stress derived from von-Mises stress, while a factor of zero represents no limiting stress. It is interesting to see that the relative SSD or RMS deviation monotonically increases with increasing limiting stress with a minimum value at no limiting stress. This suggests that the model fit is best with no fatigue limiting stress, or $\varphi = 0$.

Although this is just a numerical experiment, it does indicate that simple failure stress modification in the classical subsurface fatigue life model may not be a good option for the development of life models based on fatigue limiting stress. However, this does not imply that a fatigue stress limit does not exist. Perhaps, more extended experimental effort is necessary to establish a limiting stress and postulate a model hypothesis different from the simple stress–volume integral of classical subsurface fatigue life models.

Discussion

It is clear that the simple failure stress modification in fatigue life models is well suited for modeling the effect of residual stress in bearing races. Life predictions with modified failure stress are in good agreement with the available experimental life data. Modeling the role of a fatigue limiting stress, however, appears to be much more complicated than a simple modification of critical failure stress. Primarily due to practical limitations, full scale bearing life tests are invariably carried out at stresses much greater than the anticipated fatigue limiting stress. Thus, it is difficult to establish a fatigue limiting stress on the basis of full scale bearing life tests; likewise, it is equally difficult to rule out any existence of a limiting stress. In the event a limiting stress does exist, its implementation in life prediction models at stresses greater than the limiting stress requires a much more rigorous development of failure initiation and propagation than the simple stress function integration over a stressed volume as done in the LP model. The “numerical experiment” carried out in the present investigation simply modifies the failure stress, in an

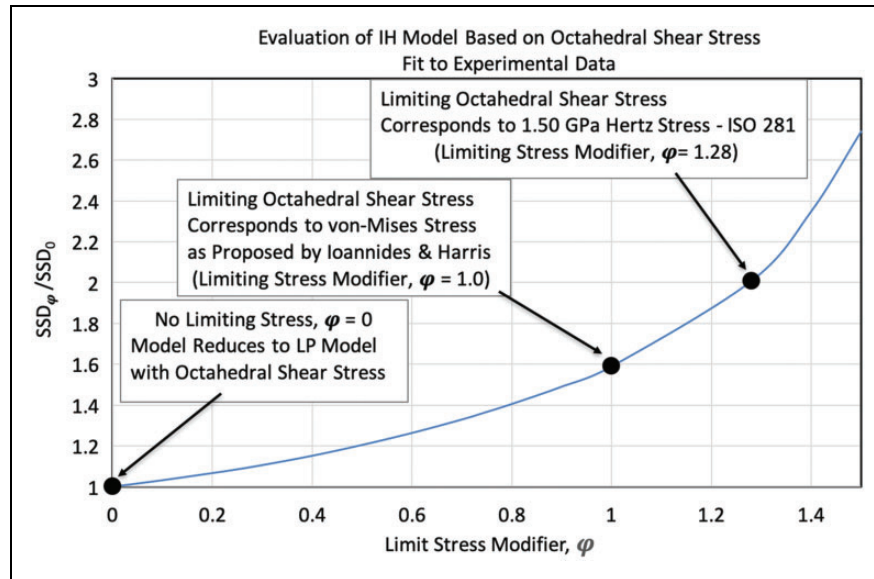


Figure 11. SSD of model predictions from experimental data for life model with fatigue limiting stress modifier, ϕ , relative to the SSD obtained with a model with no limiting stress.

LP-type model, as originally done by Ioannides and Harris,²¹ to obtain parametric life prediction as a function of the prescribed limiting stress at operating stresses greater than the limiting stress. A regression analysis of predicted lives against available experimental life data is then carried out with the hopes of estimating an optimum limiting stress. As presented above, the results of such a regression analysis show a monotonically increasing deviation between model predictions and experimental data as a function of limiting stress with the best model fit when the limiting stress is zero. Clearly, this is just a numerical exercise and by no means does it rule out an existence of a fatigue limit. Besides, the experimental data are limited and obtained over a narrow range of operating stress. However, the observation does indicate that simple failure stress modification in LP-type life models may not be realistic to implement a fatigue limiting stress for bearing life prediction at stresses greater than the limiting stress.

Unlike the well-established fatigue limiting stress in mechanical components subject to bending and/or torsion, existence of a fatigue limiting stress in rolling contacts has been a controversial subject. From an early historic perspective of rolling bearing development, Tallian³³ endorsed the fact that irrespective of operating conditions, rolling bearings will always be subjected to fatigue. With the development of more advanced bearing materials, Lamagnere et al.³⁴ have outlined fracture mechanics stages of the fatigue process, which could provide insight into a possible limiting stress below which the fatigue process could be arrested. Shimizu³⁵ and Zaretsky,³⁶ on the other hand, have maintained the existence of the fatigue process at all stress levels. Takemura et al.³⁷ have endorsed a fatigue limiting applied contact stress in the range of 1.1 to 1.7 GPa, depending on the structural cleanliness

of the material. The ISO suggested limit of 1.5 GPa³⁰ certainly falls in this range. A more recent review of the fatigue life models is presented by Sadeghi et al.³⁸ A fracture mechanics concept in which the growth of micro cracks leading to fatigue failures could be arrested has been presented by Donzella and Petrogalli.³⁹ More recently, Lewis and Tomkins,⁴⁰ along with extensive review of the recent developments related to fatigue limiting stress, have presented a fairly rigorous fracture mechanics approach to rolling bearing fatigue. Fatigue life is segmented into three parts: subsurface crack initiation, crack growth, and final propagation to form a spall. It is postulated that micro cracks initiate at one or both ends of a non-metallic inclusion; the cracks grow parallel to the surface forming a “butterfly” pattern, and eventually propagate to the surface resulting in a failure. A possible limiting stress, below which no crack initiation may occur, is related to size of the inclusion. A more conservative limiting stress below which crack growth could be arrested is also proposed. Very recently, with due recognition of the fact that experimental determination of applicable fatigue limiting stress may be impractical and perhaps expensive, Allison and Pandkar⁴¹ undertook a finite element analysis to model the role of non-metallic inclusions in the material matrix in defining a possible limiting stress. It is postulated that these inclusions act as stress risers, accumulate micro-plastic strain, and eventually lead to micro-crack initiation, and eventual bearing failure. A fatigue limiting stress is then interpreted as a stress below which no local yielding may occur. In addition to the limiting stress dependence on inclusion size and properties, as pointed out by Lewis and Tomkins,⁴⁰ stress concentration resulting from debonded inclusions and thermal dependence of elastic modulus are identified as the key factors which define a limiting stress.

In absence of any limiting stress, as demonstrated in Figure 5, bearing life predictions by the current LP and GZ life models, respectively, increase by factors of about 20 and 60 when the applied contact stress reduces from 2 GPa, which is a typical lower bound for current bearing tests, to the ISO proposed limiting stress of 1.5 GPa. Such an observation implies that just to validate the current models at 1.5 GPa, the test duration, a current upper bound on which is presently about 5000 hours, will have to be increased far beyond any practical limits. Thus, both the acceptance and rejection of a possible fatigue limiting stress are beyond the practical limitations of full scale bearing life tests. While there has been significant development in fracture mechanics approaches to understanding the origination and propagation of fatigue cracks as a function of material structure, computational models are still restricted to Weibull^{1,2} and Lundberg and Palmgren^{3,4} type formulations where life is defined as a function of a stress function integration over the stressed volume with a Weibull-type statistical variance. The effect of material structure and operating conditions, such as lubrication, are implemented in terms of life modification factors²⁹⁻³¹ applied over the computed basic life. With significant advancement in materials used for rolling bearing applications, the next step is to formulate new life models which not only implement any possible fatigue limiting stress but quantify the micro crack initiation, growth and propagation processes, as outlined by Lewis and Tomkins,⁴⁰ to compute life of the bearing when the applied contact stress is greater than the possible limiting stress. It should be noted that while dynamic stresses in the bearing races may overcome any stresses, which lead to arrest of crack growth, and significantly reduce fatigue life, compressive residual stresses may significantly retard or completely arrest crack growth and propagation, and thereby provide infinite life. It is therefore necessary to superimpose these stresses on the subsurface stress field generated by the applied loading. Perhaps, the finite element formulation of Allison and Pandkar⁴¹ may be extended to provide required superimposition of stresses. Life predictions obtained with such sophisticated models may certainly be evaluated against experimental life data obtained by carrying out full scale bearing life tests, under the current experimental framework.

Summary

The current development presents an approach for failure stress modification in the generalized subsurface rolling contact fatigue life models. In particular, the following has been accomplished:

1. A procedure has been developed to modify the failure stress in the generalized models to model the effect of residual and hoop stresses. Parametric

evaluation of the Gupta-Zaretsky (GZ) model demonstrates significant life enhancement as a result of compressive residual stress. The equivalent life modification factor is both residual stress and applied load dependent. At light loads, even relatively low levels of compressive residual stress may contribute to significant increase in fatigue life. The enhanced model also leads to infinite life when the maximum subsurface shear stress resulting from applied load on the bearing is less than that produced by the compressive residual stress.

2. Life predictions obtained by the enhanced model are in good agreement with available experimental data for a 40-mm angular contact ball bearing with M50-NiL races and silicon nitride balls.
3. The failure stress modification is also applied to implement a fatigue limiting stress as done by Ioannides and Harris (IH). The IH model, as implemented in the present work, is based on the Lundberg-Palmgren (LP) model with the orthogonal shear stress replaced by octahedral shear stress, a limiting value for which is related to the von-Mises stress of the bearing material. The empirical model constant is derived by least-squared regression of model predictions, against available experimental life data. A limiting stress is then applied to model life over a range of applied contact stress. Parametric results are obtained with varying levels of limiting stress, including the recommendation in ISO 281. While the model converges to LP predictions with no limiting stress, the predicted lives are orders of magnitude higher at light loads.
4. As an alternate implementation of fatigue limiting stress, the model constant at any prescribed limiting stress is independently computed by regression against available experimental life data. Parametric life predictions are then made as a function of applied load or contact stress in the bearing. While the solutions, with no limiting stress, again converge to LP predictions, the limiting stress-based models show very large increase in life at light loads, while the predicted life is greatly reduced at high loads. The increase in predicted life is largest with the ISO 281 suggested limiting stress. These results are qualitatively similar to those published by Ioannides and Harris for rotating beams.
5. Evaluation of the computed sum of squared deviation between model predictions and experimental life data as a function of limiting stress suggests that the fit is best at no fatigue limiting stress. This leads to the conclusion that the simple failure stress modification in current life models, based on the subsurface fatigue hypothesis of Lundberg and Palmgren, may not be appropriate to model life enhancement as a result of any fatigue limiting stress. Perhaps, more advanced fracture mechanics-based life model formulations are necessary to model the role of a possible fatigue limiting stress.

Declaration of Conflicting Interests

The author(s) declared no potential conflicts of interest with respect to the research, authorship, and/or publication of this article.

Funding

The author(s) disclosed receipt of the following financial support for the research, authorship, and/or publication of this article: US Air Force Small Business Innovation Research (SBIR) Phase II (Contract #FA8650-15-C-2534) contract awarded to PKG Inc. The Air Force Technical Contract Monitor was Jeremy Nickell. Supporting information on experimental data was provided by Hitesh K. Trivedi of UES Inc.

References

- Weibull W. A statistical theory of the strength of materials. *Ingeniors Vetenskaps Adademien (Proc Royal Swedish Academy of Engineers)* 1939; 151.
- Weibull W. The phenomenon of rupture. *Ingeniors Vetenskaps Adademien (Proc Royal Swedish Academy of Engineers)* 1939; 153.
- Lundberg G and Palmgren A. Dynamic capacity of rolling bearings. *Acta Polytech Mech Eng* 1947; Series 1, Nos. 3, 7, Royal Swedish Acad. Eng.
- Lundberg G and Palmgren A. Dynamic capacity of roller bearings. *Acta Polytech Mech Eng* 1952 Series 2, No. 4, 96, Royal Swedish Acad. Eng.
- Gupta PK and Zaretsky EV. New stress based fatigue life models for ball and roller bearings. *STLE Tribol Trans* 2018; 61: 304–324.
- Zaretsky EV. Fatigue criterion to system design, life and reliability. *AIAA J Propuls Power* 1987; 107: 76–83.
- Zaretsky EV. Rolling bearing life prediction, theory and application. In: Nikas GK (ed) *Recent developments in wear prevention, friction and lubrication*, Chapter 2. Kerala, India: Research Signpost, 2010, pp.45–136.
- Almen JO. Effects of residual stress on rolling bodies. In: Bidwell JB (ed) *Rolling contact phenomena*. New York: Elsevier Publishing Company, 1962, pp.400–424.
- Bush JJ, Grube GH and Robinson GH. Microstructural and residual stress changes in hardened steel due to rolling contact. In: Bidwell JB (ed) *Rolling contact phenomena*. New York: Elsevier Publishing Company, 1962, pp.365–399.
- Koistinen DP. The generation of residual compressive stresses in the surface layers of through-hardened steel components by heat treatment. *ASM Trans* 1964; 57: 581–588.
- Gentile AJ, Jordan EF and Martin AD. Phase transformations in high-carbon, high-hardness steels under contact loads. *AIME Trans* 1965; 233: 1085–1093.
- Gentile AJ and Martin AD. The effect of prior metallurgically induced compressive residual stress on the metallurgical and endurance properties of overload tested ball bearings. *ASME Paper* 65-WA/CF-7, 1965.
- Parker RJ and Zaretsky EV. *Effect of residual stresses induced by prestressing on rolling-element fatigue life*. NASA TN D-6095, 1972.
- Lorosch HK. Influence of load on the magnitude of the life exponent for rolling bearings. In: Hoo JJC (ed) *Rolling contact fatigue testing of bearing steels*. ASTM STP-771, Philadelphia, PA: American Society for Testing and Materials, 1982, pp.275–292.
- Zwirlein O and Schlicht H. Rolling contact fatigue mechanisms-accelerated testing versus field performance. In: Hoo JJC (ed) *Rolling contact fatigue testing of bearing steels*. ASTM STP-771, Philadelphia, PA: American Society for Testing and Materials, 1982, pp.358–379.
- Bamberger EN and Kroeger DJ. *Rolling element fatigue life of a carburized modified m-50 bearing steel*, NASA CR-168295, 1984.
- Townsend DP and Bamberger EN. Surface fatigue life of carburized and hardened M50-NiL and AISI 9310 spur gears and rolling-contact test bars. *J Propulsion Power* 1991; 7: 642–649.
- Kotzalas M. A theoretical study of residual stress effects on fatigue life prediction. *STLE Tribol Trans* 2001; 44: 609–614.
- Rosado L, Forster NH, Thompson KL, et al. Rolling contact life and spall propagation of AISI M50, M50-NiL and AISI 52100, Part I: Experimental results. *STLE Tribol Trans* 2010; 53: 29–41.
- Oswald FB, Zaretsky EV and Poplawski JV. Relation between Residual and hoop stresses and rolling bearing fatigue life. *STLE Tribol Trans* 2014; 57: 749–765.
- Ioannides E and Harris TA. New fatigue life model for rolling bearings. *ASME J Lubr Technol* 1985; 107: 367–378.
- Harris TA and McCool J. On the accuracy of rolling bearing fatigue life prediction. *ASME J Tribol* 1996; 118: 297–310.
- Harris TA and Kotzalas MN. *Rolling bearing analysis – fifth edition – advanced concepts of bearing technology*. Boca Raton: CRC Taylor & Francis, 2007, p.253.
- Gupta PK. *Advanced dynamics of rolling elements*. New York: Springer-Verlag, 1984.
- Klecka MA, Subhash G and Arakere NK. Micro-structure property relationships in M50-NiL and P675 case hardened bearing steels. *STLE Tribol Trans* 2013; 56: 1046–1059.
- Londhe ND, Arakere NK and Subhash G. Extended Hertz theory contact mechanics for case-hardened steels with implications for bearing fatigue life. *ASME J Tribol* 2018; 140: Article #021401 (11 pages).
- Material Data Sheet, Latrobe Lescalloy, M-50 VIMVAR, www.matweb.com (accessed 31 August 2018).
- Trivedi HK, Rosado L, Gerandi DT, et al. Fatigue life performance of hybrid angular contact Pyrowear 675 bearings. In: Beswick JM (ed) *Bearing and steel technologies*, 11th volume, Progress in Steel Technologies and Bearing Steel Quality. ASTM STP1600, West Conshohocken, PA: ASTM International, 2017, pp.275–299.
- ISO. *Rolling bearings – dynamic load ratings and rating life*. International Standard ISO/DIS 281. Geneva, Switzerland: International Standards Organization, 1989.
- Zaretsky EV. *STLE life factors for rolling bearings*. Park Ridge, IL: STLE, 1992.
- Tallian TE. A data-fitted rolling bearing life prediction model for variable operating conditions. *STLE Tribol Trans* 1999; 42: 241–249.

32. ISO 281:2007. *Rolling bearings – dynamic load ratings and rating life*. Geneva: International Organization for Standardization, 2007.
33. Tallian T. *Progress in rolling contact technology*. Report AL690007. King of Prussia, PA: SKF Industries, Inc., 1969.
34. Lamagnere P, Fougeres R, Lormand G, et al. A physically based model for endurance limit of bearing steels. *ASME J Tribol* 1998; 120: 421–426.
35. Shimizu S. Fatigue limit concept and life prediction model for rolling contact machine elements. *STLE Tribol Trans* 2002; 45: 39–46.
36. Zaretsky EV. In search of a fatigue limit: a critique of ISO standard 281:2007. *STLE Tribol Lubr Technol* 2010; 66: 30–40.
37. Takemura H, Matsumoto Y and Marakami Y. Development of new life equation for ball and roller bearings. *NSK Motion Control* 2001; 11: 1–10.
38. Sadeghi F, Jalalahmadi B, Slack TS, et al. A review of rolling contact fatigue. *ASME J Tribol* 2009; 131: Article # 041403 (15 pages).
39. Donzella G and Petrogalli C. A failure assessment diagram for components subjected to rolling contact loading. *Int J Fatigue* 2010; 32: 256–268.
40. Lewis MWJ and Tomkins B. A fracture mechanics interpretation of rolling bearing fatigue. *Proc IMechE, Part J: J Engineering Tribology* 2012; 226: 389–405.
41. Allison B and Pandkar A. Critical factors of determining a first estimate of fatigue limit of bearing steels under rolling contact fatigue. *Int J Fatigue* 2018; 117: 396–406.

Appendix

Notation

a	major contact half width (m)
a^*	dimensionless major contact half width for point contact
A_{LP}	empirical constant in LP dynamic stress capacity equation (units depend on exponent c and h , default value = $1.4599 \times 10^9 \text{ N/m}^{1.933}$)
A_{GZ}	empirical constant in GZ dynamic stress capacity equation (units depend on exponent c , default value = $6.4229 \times 10^8 \text{ N/m}^{1.777}$)
A_{IH}	empirical constant in IH dynamic stress capacity equation (units depend on exponent c and h , default value = $1.5524 \times 10^9 \text{ N/m}^{1.933}$)
b	minor contact half width (m)
b^*	dimensionless minor contact half width for point contact
c	critical failure stress exponent (default value = 31/3)

d	contact track diameter on race (m)
D	rolling element diameter (m)
E	modulus of elasticity (Pa)
E'	effective elastic modulus parameter for contacting surfaces (Pa)
G	geometric parameter in dynamic stress capacity equation (units depend on exponent c and h)
K	proportionality constant in fundamental life equation (units depend on exponent c and h)
h	critical failure stress depth exponent (default value = 7/3)
L	fatigue life (h)
m	Weibull slope (default value = 10/9)
p_H	maximum Hertz contact stress (Pa)
p_{Hc}	dynamic stress capacity (Pa)
S	cumulative survival probability
u	number of stress cycles per revolution of rotating race
V_o	stressed volume with maximum orthogonal shear stress (m^3)
V_m	stressed volume with maximum shear stress (m^3)
ζ	ratio of critical failure stress to maximum Hertz contact stress
η	ratio of effective contact width to major contact half width
κ	model constant
λ_E	material parameter (ratio of E' to E'_{52100})
$\sum \rho$	curvature sum of contacting surfaces (1/m)
σ_r	residual stress (Pa)
σ_h	hoop stress (Pa)
σ_v	von-Mises stress (Pa)
τ_o	maximum orthogonal shear stress (Pa)
τ_m	maximum shear stress (Pa)
τ_e	equivalent maximum shear stress due to residual and hoop stresses (Pa)
τ_l	limiting shear stress (Pa)
τ_{oct}	maximum octahedral shear stress (Pa)
ν	Poisson's ratio
φ	fatigue limiting stress modifier
Φ	dynamic stress capacity adjustment factor
ξ	ratio of depth of critical failure stress to contact minor half width
ψ_R	residual stress life factor
ψ_S	fatigue limiting stress life factor
ω_b	rolling element angular velocity (rad/s)
$\dot{\theta}$	Rolling element orbital velocity (rad/s)
Ω	race angular velocity (rad/s)